Anal Bioanal Chem (2010) 397:2143–2148
DOI 10.1007/s00216-010-3696-6

ORIGINAL PAPER

3D visualization of the microstructure of *Quedius beesoni* Cameron using micro-CT

Kai Zhang · De-e Li · Peiping Zhu · Qingxi Yuan · Wanxia Huang · Xiaosong Liu · Youli Hong · Gun Gao · Xin Ge · Hongzhang Zhou · Ziyu Wu

Received: 9 January 2010 / Revised: 26 March 2010 / Accepted: 29 March 2010 / Published online: 30 April 2010

Abstract The investigation of the internal morphology of insects is usually performed using classical microtomy yielding optical micrographs of stained thin sections. The achievement of high-quality cross sections for microtomy is time-consuming and the risk of damaging sections is unavoidable. Moreover, the approach is impractical, in particular when quick acquisition of 3D structural information is required. Recently, X-ray computed microtomography (micro-CT) with a high spatial resolution was considered as a potential tool for the morphological classification of insects. We used micro-CT to investigate *Quedius beesoni* Cameron at the cellular length scale. This method provides a new powerful and nondestructive approach to obtain 3D structural information on the biological organization of insects. The preliminary images presented in this contribution clearly reveal the endoskeleton and the muscles of the head and the thorax with a full 3D structure. We also reconstructed the 3D structure of the brain of *Quedius beesoni* Cameron, and this is the first reconstruction in Staphylinidae, which will be a great advancement for morphological and phylogenic research. We claim that both the spatial resolution and the contrast characteristic of micro-CT imaging may fulfill the requirements necessary for zoological insect morphology and phylogeny, in particular, when a classification of a rare and unique insect specimen is required.

Keywords Tomography · Staphylinidae · Morphology · X-ray image

K. Zhang · P. Zhu · Q. Yuan · W. Huang · X. Liu · Y. Hong · Z. Wu (✉)
Beijing Synchrotron Radiation Facility, Institute of High Energy Physics, Chinese Academy of Sciences,
Beijing 100049, China
e-mail: wuzy@ustc.edu.cn

D.-e. Li · H. Zhou (✉)
Key Laboratory of the Zoological Systematics and Evolution,
Institute of Zoology, Chinese Academy of Sciences,
Beijing 100101, China
e-mail: zhouhz@ioz.ac.cn

G. Gao · X. Ge · Z. Wu
National Synchrotron Radiation Laboratory,
University of Science and Technology of China,
Hefei 230026, China

Introduction

For insect morphology, the insect is a complex biological system characterized by several hierarchical levels of organization. Structural features from the macroscopic to the submicroscopic scale are necessary and contribute to the morphological classification of insects. In particular, the measurement of volume structures is critical to understand features and evolution of insects. Various imaging techniques are typically used, such as microtomy, which yields optical micrographs of stained thin sections, and electron microscopy which allows the highest magnifications, providing a close qualitative insight of the 3D structure of a specimen. Although a lot has been learned through these methods, both techniques are sometimes impractical because of the time they require to investigate an insect, difficulties and efforts associated with the sample preparation, and the unavoidable risk of damage during the preparation of a thin section. Furthermore, for both methods because of the limited penetration depth of electrons, the 3D observation is limited to the *Z*-direction (i.e., in the direction of the incoming beam) to several tens of micrometers. Therefore, a high-resolution, nondestruc-

tive, 3D imaging procedure such as X-ray computed microtomography (micro-CT) has recently been considered suitable for such research.

Micro-CT is an entirely nondestructive imaging method that does not require slicing or a specimen to be cut [1]. A series of noninvasive views through the sample (i.e., radiographic projections recorded from different viewing angles) are reconstructed mathematically into transverse 2D cross sections, and with dedicated software protocols, detailed 3D images can be obtained. Besides the marked advantage of a 3D perspective, the technique also achieves a significant improvement in resolution, allowing small specimen imaging with a spatial resolution in the range 1–50 μm, enough to distinguish the cell structure, although at a rather coarse scale [2]. This technique is, however, continuously being improved and both improved image quality and higher spatial resolution will certainly be achieved in the next few years. In addition, micro-CT is also cost-effective because it requires minimal sample preparation and relatively simple data postprocessing. Recent developments have extended its range of application to vascular studies and to the characterization of the phenotype of transgenic and knockout animal models during preclinical investigations [3–5]. Owing to the accessibility to quantitative 3D data, micro-CT will soon probably become the standard tool in many laboratories. Here, we will demonstrate how micro-CT may become a unique and effective tool for insect morphology.

Quedius beesoni Cameron is a rove beetle species of the family Staphylinidae (Insecta, Coleoptera). Staphylinidae is one of the largest beetle families and is very important for understanding beetle speciation and morphological diversification [6]. Rove beetle morphology is usually studied with conventional tools such as light microscopes and electron microscopes [4, 7–11]. Light microscopes are limited by amplification rates, whereas scanning electron microscopes can be used to observe surface structures[4, 10, 11]. Micro-CT is a great tool to study insect morphology [12–14]. Pioneer research appeared even in rove beetle studies [15]; however, these studies were based on 2D pictures, with no 3D digital reconstructions of the insect anatomy. In our work we used the micro-CT method to study the morphology of *Quedius beesoni* Cameron, with emphasis given to the 3D digital reconstruction of body structures, especially some important inner organs.

Material and methods

Sample preparation

The specimens of *Quedius beesoni* Cameron we used were collected by H.Z. Zhou from the Taibai Mountain, Shaanxi province, China. Specimens (stored in 75% alcohol or attached to pine labels) were preserved in the Institute of Zoology of the Chinese Academy of Sciences. For morphological dissection, specimens were relaxed in warm water (60 °C) for about 0.5–1 h, then elytra, hindwing, and metanotum were removed to observe muscles and endoskeleton. Specimens were cleared in 10% KOH for 5 min or more until the mouthparts were soft enough for easy dissection and examination under a microscope. After examination, body parts were preserved permanently in glycerin for future studies. Observations were done under a compound microscope (ZEISS STEMI-2000C) to corroborate and complement the X-ray data. For the micro-CT, we fixed specimens with Dubosque-Brazil for 2 days, then transferred them to 100% alcohol gradually, and dried them in a critical point dryer (HCP-2). Finally, the dry specimens were mounted with gluewater on the sample stage of the X-ray machine.

Arrangement of the X-ray computed microtomography experiment

All measurements and reconstructions were performed at the Institute of High Energy Physics of the Chinese Academy of Sciences using the MicroXCT-200 system, manufactured by Xradia (USA). The typical MicroXCT 200 system shown in Fig. 1 consists of a sealed microfocus X-ray tube (40 kV, 250 μA, 5-um spot size), a fiber-optic coupling, a cooled CCD-detector, and a precision object manipulator. A dual-processor computer was also used to steer the stepping motors, axial shift, and data recording, as well as to reconstruct the CT images. The basic principles of this system are similar to those used in medical CT scanners. However, recent improvements in the development of X-ray sources and CCD detectors now make it possible to achieve a resolution of a few microns. In the experiment, the photon energy used was 40 kV and the object-to-detector distance was 15 mm. Further, the detection chain consists of a 20-μm YAG:Ce scintillator, an optical microscope (with the magnification ranging between 1 and 40), and a low-noise fast-readout CCD of 2,048×2,048 pixels and

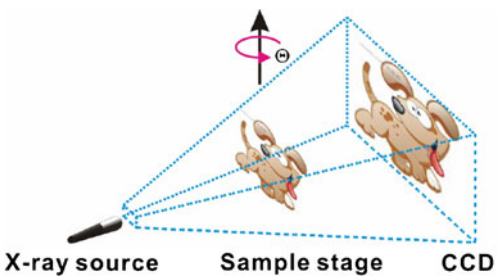

Fig. 1 Layout of the X-ray computed microtomography system

16-bit dynamic range. To get the 3D inner structure of *Quedius beesoni* Cameron, a magnification factor of 4 was used, corresponding to effective pixels of 3 μm.

The experiment was performed by placing the object on the specimen stage between the X-ray source and the CCD detector. As the source produces a conical beam of X-rays, magnification is achieved by moving the object toward the X-ray source. After the positioning, 2D X-ray images with an exposure time of 10 s per image were acquired from 361 angles over 180°, and were saved in the computer memory. The total exposure time and the scan time were 60 and 70 min, respectively. Then cross sections of the object were reconstructed by applying the "filtered back-projection algorithm for fan-beam geometries." This algorithm combines all angular information for every line in the camera to generate a cross section of the object. With this method we could reconstruct up to 1,024 cross sections of the object, with a lateral resolution and a slice-to-slice distance of a few microns. During the slice reconstruction, a correction was made to reduce the effects of beam hardening, which is caused by an apparent higher X-ray attenuation near the periphery of an otherwise homogeneous sample. Finally, the 3D reconstruction and analysis of the X-ray data was done with the Amira 4.1 software package on a Xeon 2660 MHz computer. The Amira 4.1 software package allows the recombination of the X-ray sections into a 3D model of the object. This model can be manipulated in different ways. It is possible to rotate the model around all three axes and change the magnification. One can also remove parts of the dataset to look into the beetle. Since the X-ray data only represent absorption values, it is necessary to apply "false" color tables to the dataset to produce grayscale or color images. Via the color tables, it is also possible to change the opacity of selected colors or absorption values.

Results

After the experiments, the microstructure of the specimens was observed and measured using the visualization and measuring features of the Amira 4.1 software package. Figure 4d and e shows examples of the transverse cross sections of *Quedius beesoni* Cameron, respectively, and the 3D reconstruction is shown in Figs. 2, 3d–f, and Fig. 4a–c.

From Fig. 2a it can be clearly seen that the spatial resolution already differentiates individual segments of insects, namely, the locomotion segments prothorax, mesothorax, and metathorax with their legs and wing muscles, and the abdomen with the intestine and the female reproductive system. But with use of only a single 2D projection it is impossible to recognize the muscles of the prothorax, mesothorax, and metathorax, because the overlap of projections of complex features complicates the analysis of an image. To distinguish the precise interior structures of *Quedius beesoni* Cameron, slice images and a 3D rendering of the samples were necessary. Figure 2 shows a complete body of *Quedius beesoni* Cameron in dorsal, lateral, and ventral views, which clearly revealed the shape and location of the inner organs. From these images

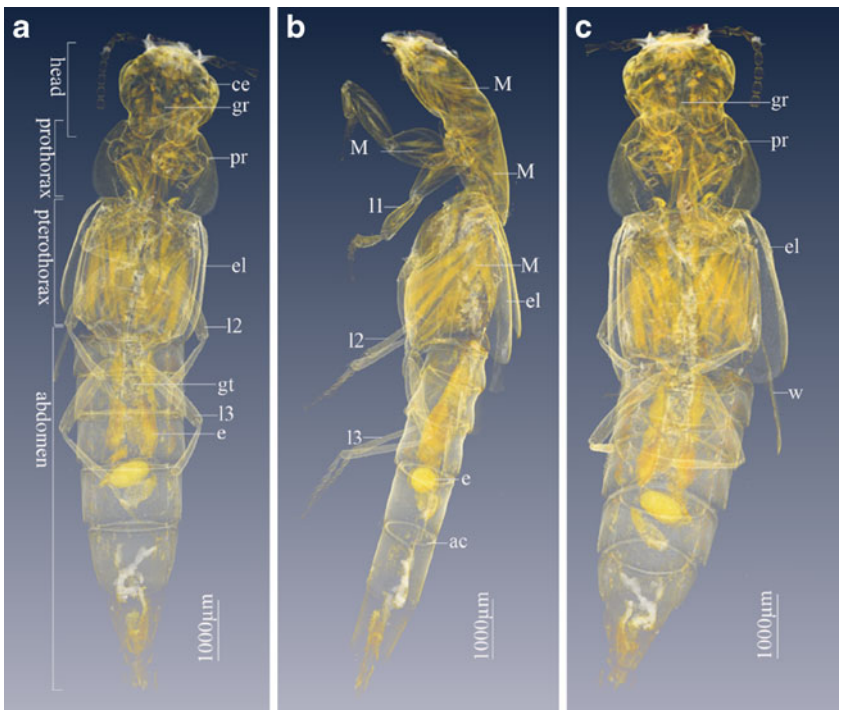

Fig. 2 *Quedius beesoni* Cameron, 3D reconstruction: a ventral view; b lateral view; c dorsal view. *ac* antecosta, *ce* compound eyes, *e* egg, *el* elytra, *gr* gular ridge, *gt* gut tube, *l1* proleg, *l2* mesoleg, *l3* metaleg, *M* muscles, *pr* pleural ridge, *w* hindwing

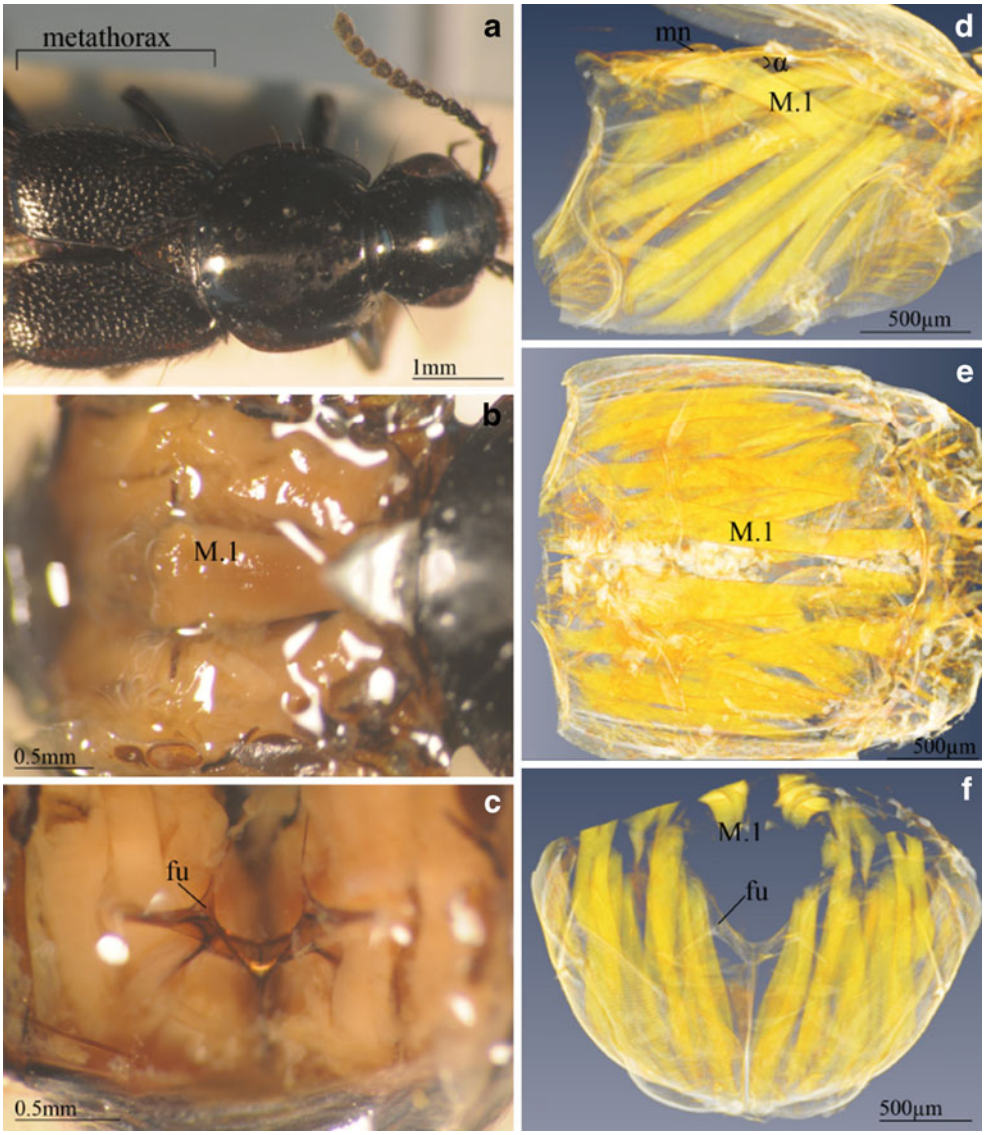

Fig. 3 *Quedius beesoni* Cameron. **a-c** Optical images: a head and thorax; b metathorax by removing wings and metanotum; c metathorax by removing wings, metanotum, and some muscles. **d-e** 3D reconstructions: d metathorax, lateral view by cutting off the right part; e metathorax, dorsal view by cutting off the wings and metanotum; f posterior view of the metathorax. *fu* metafurca, *M.1 musculus metanoti primus*, *mn* metanotum, α angle between *musculus metanoti primus* and metanotum

we can observe most body parts of the beetle: compound eyes, head and thorax muscles, proleg, mesoleg, and metaleg, elytra, eggs, gut tube, and some of the endoskeleton. In the female beetle in Fig. 2, we can also observe well-developed ovaries, with eggs situated at each side of the gut tube within the abdomen. The endoskeleton is for the attachment of muscles. The images show that gular ridges under the head are well developed and separated from each other (Fig. 2a). The hypomeron of the prothorax is separated into two parts by the pleural ridges (Fig. 2a). The antecosta of the abdominal segments are well developed as the attachment of abdominal muscles (Fig. 2a, c). The 3D structure of the metathorax is also shown in Fig. 3d–f, which can be compared with the optical images of the same structure obtained using the optical microscope method (Fig. 3a–c) . Obviously, the micro-CT method with 3D morphological reconstruction displayed multiple advantages in insect morphology studies. It can directly image insect structures and obtains 3D representations of different structures, especially for the delicate micromorphological structures, and does not dissect or destroy samples or specimens. This is highly beneficial especially for taxonomists; they have to preserve permanently some valuable specimens of scientific importance (e.g., the type specimens). With the optical microscope method, however, dissection and destruction of specimens are normal and cannot be avoided. In addition, use of the optical microscope method to study insect morphology can only be conducted by skilled technicians with long-term training and qualifications. However, the micro-CT method is highly dependent on modern and complicated equipment of high cost. From Fig. 3, we can also see clearly that the optical microscope images show some internal structures such as muscles (e.g., *musculus metanoti primus*), but these are not as good as the images from the micro-CT method in displaying the microstructures themselves and their orien-

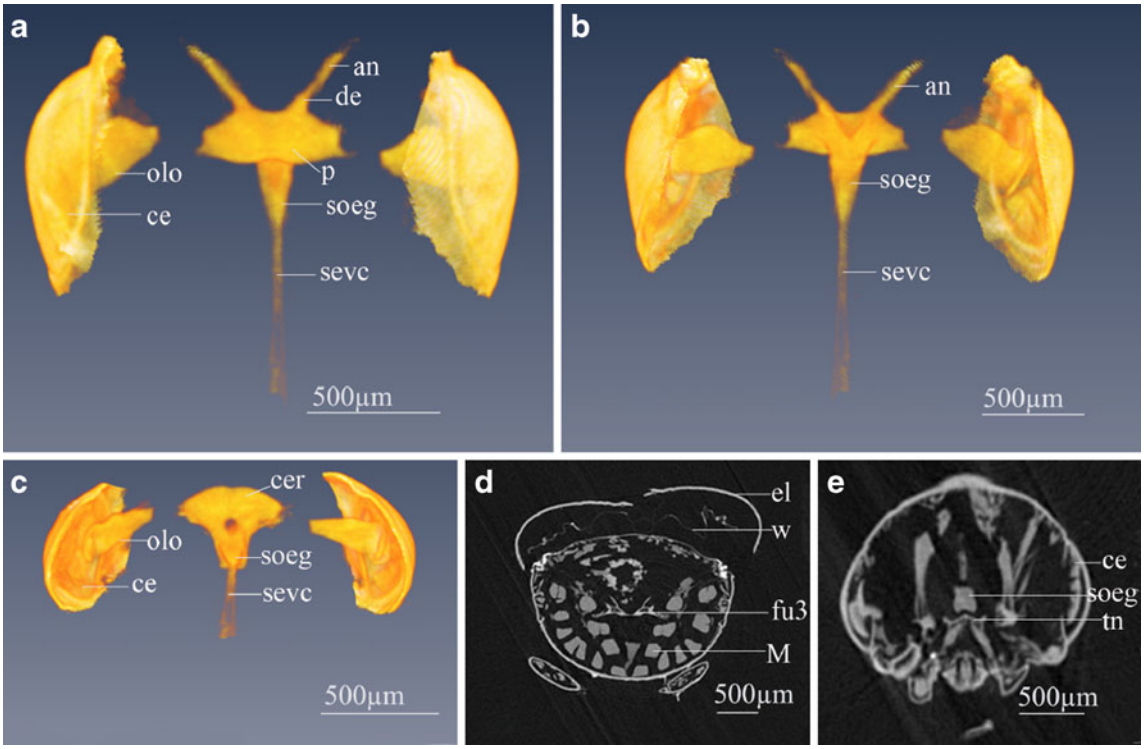

Fig. 4 *Quedius beesoni* Cameron. **a–c** 3D reconstructions. d The 77th slice. e The 378th slice. *an* antennal nerve, *ce* compound eye, *cer* brain, *de* deutocerebrum, *el* elytra, *fu3* metafurca, *M* muscles, *tn* tentorium, *olo* optical lobe, *p* protocerebrum, *soeg* subesophageal complex, *sevc* connectives, *w* hindwing

tations. Moreover, some very fine structures attached to external skeletons are often destroyed and even lost in dissecting processes. This has long affected the studies of entomologists. We select as an example the *musculus metanoti primus*, which acts as a hindwing depressor. From Fig. 3d we can measure its length and angle, whereas from optical images (Fig. 3b, c) we may obtain only its length. Combining its orientation with the orientations of other muscles which contribute to the hindwing movements, we may calculate the dynamics of the hindwing.

In this study, the 3D structure of the brain of *Quedius beesoni* Cameron was also reconstructed. Figure 4 displays the reconstructed 3D structures of the brain of *Quedius beesoni* Cameron: protocerebrum, deutocerebrum, optical lobe, subesophageal complex, antennal nerve, connectives, and compound eyes. From slice pictures (Fig. 4d, e), we can also observe the compound eyes, the subesophageal complex, the tentorium, the metafurca, and the hindwing. The intrinsic muscles of the foreleg can be clearly recognized in Fig. 4b. The brain of *Quedius beesoni* Cameron is relatively small in comparison with the size of the head (Fig. 2a–c). It is situated in the anterior part of the head, above the tentorium and between the compound eyes (Figs. 2a–c, 4a–c). Most rove beetles (Staphylinidae) are predators and have well-developed mouthparts and sense organs. The nerves controlling these organs are also very well developed. The antennal nerves controlling the movement and sensors of the antennae are thick (Fig. 3a–c). The compound eyes of this rove beetle are large compared with the head, so the optical lobes, which contain the eye nerve roots, are broad and flat (Fig. 4a–c). The subesophageal complex is connected to the brain by circumoesophageal connectives that form a round circle through which the foregut passes (Fig. 4c). The subesophageal complex extends to the rear between gular ridges and has connections with the prothorax ganglion. It also extends anteriorly with several pair of nerves into mouthparts. In Fig. 4e we can see around the subesophageal complex muscles and tentorium. Reconstructed 3D models of these internal structures let us clearly observe the morphology of *Quedius beesoni* Cameron. The latter will be helpful to understand the morphological adaptation and the evolution of beetles. Moreover, micro-CT and 3D reconstruction can also be used in morphometric studies when we want to make a geometric analysis and to compare beetle structures quantitatively.

From the above analysis, we can see that micro-CT imaging provides a huge amount of useful experimental data. Such images through the body of an insect show structural details down to muscles and endoskeleton. The details are in precise structural agreement with those

reported in the literature, based on histological sections. The presently achieved spatial resolution was obtained in a fast and nondestructive way. Moreover, micro-CT also provides the possibility to explore the internal 3D microstructure of the insect morphology. By stacking sequences of micro-CT slices, we can obtain 3D rendering, revealing the complexity of the distribution of thoracic muscles. All these advantages make micro-CT a new powerful tool for the morphological classification of insects with high spatial resolution. The main drawback of micro-CT is the weak X-ray absorption of the transparent thin tissues. Recently, a new method has been introduced that shows promising results in the practical use of X-ray phase contrast imaging. It is based on the consequences of the refraction of X-rays (resulting from the slightly different velocities of X-ray photons through different media, similarly to the different refraction of light) within tissues [16–22]. The method offers a tenfold or higher increase of the density resolution of soft tissues over the current attenuation-based imaging method, but it also has the potential for reduced radiation exposure because the signal is associated with the phase shift or refraction of individual photons rather than with the reduction of the photon flux. Combining this technology with a brilliant synchrotron radiation source, synchrotron radiation micro-CT systems may transform our capability to visualize and reconstruct 3D structures down to the nanometer level [23–27].

Conclusion

Time-consuming and complex procedures are necessary to obtain specimen cross sections for microtomy. The use of optical micrographs is impractical for a 3D structural reconstruction of a specimen in a short period of time. We presented here images based on experiments of micro-CT that overcomes the drawbacks and limitations of classic microtomy. We presented and discussed the internal 3D structure of *Quedius beesoni* Cameron, for which the reconstruction revealed the differentiation of fine structural and morphological details such as the musculature system, the brain, and the subesophageal complex. The present investigation also demonstrated that micro-CT is able to provide the spatial resolution necessary for the investigation of insect morphology. The spatial resolution at the level required by zoologists is compatible with that of conventional invasive light microscope techniques. However, it is also accessible to micro-CT with technical modifications of standard in vivo animal scanners and within reasonable experimental times. In conclusion, this investigation demonstrates that micro-CT can successfully be used for the study of the morphology of insects in particular to clarify the 2D and/or the 3D reconstruction of their internal structures.

Acknowledgements This work was partly supported by the National Outstanding Youth Fund (project no. 10125523 to Z.W.), the Knowledge Innovation Program of the Chinese Academy of Sciences (KJCX2-YW-N42), the Key Important Project of the National Natural Science Foundation of China (10734070), the National Natural Science Foundation of China (NSFC 10774144 and 10979055), and the National Basic Research Program of China (2009CB930804).

References

1. Hounsfield G (1973) Br J Radiol 46:1016
2. Peyrina F, Salomea M, Cloetensb P et al (1998) Technol Health Care 6:391–401
3. Holdsworth D, Thornton M (2002) Trends Biotechnol 20:34–39
4. Betz O, Thayer M, Newton A (2003) Acta Zool 84:179–238
5. Jorgensen S, Demirkaya O, Ritman E (1998) Am J Physiol Heart Circ Physiol 275:H1103
6. Herman L (2001) Catalog of the Staphylinidae (Insecta: Coleoptera): 1758 to the end of the second millennium. American Museum of Natural History, New York
7. Blackwelder R (1936) Smithson Misc Collect 94:1–102
8. Naomi S (1987) Jpn J Entomol 55:450–458
9. Naomi S (1989) Jpn J Entomol 57:82–90
10. Betz O (1996) Zoomorphology 116:15–34
11. Kölsch G, Betz O (1998) Zoomorphology 118:263–272
12. Gorb S, Beutel R (2000) J Morphol 244:1–14
13. Hörnschemeyer T, Beutel R, Pasop F (2002) J Morphol 252:298–314
14. Beutel R, Ge S, Hörnschemeyer T (2008) Cladistics 24:270–298
15. Weide D, Betz O (2009) J Morphol 270:1503–1523
16. Zhu PP, Wang JY, Yuan QX et al (2005) Appl Phys Lett 87:264101–264103
17. Wang J, Zhu P, Yuan Q et al (2006) Phys Med Biol 51:3391–3396
18. Chapman D, Thomlinson W, Johnston R et al (1997) Phys Med Biol 42:2015–2026
19. Momose A (2002) J Synchrotron Radiat 9:136–142
20. Wilkins S, Gureyev T, Gao D et al (1996) Nature 384:335–338
21. Davis T, Gao D, Gureyev T et al (1995) Nature 373:595–598
22. Gureyev TE, Mayo S, Wilkins SW et al (2001) Phys Rev Lett 86:5827
23. Chao W, Harteneck B, Liddle J et al (2005) Nature 435:1210–1213
24. Wieland M, Wilhein T, Spielmann C et al (2003) Appl Phys B Lasers Opt 76:885–889
25. Cloetens P, Barrett R, Baruchel J et al (1996) J Phys D Appl Phys 29:133–146
26. Lewis R (1997) Phys Med Biol 42:1213–1243
27. Kron T (1998) Phys Med Biol 43:215–216